Extended Essay

Effect of Microenvironmental pH on Catalase Kinetics:

MODELLING ENZYMATIC FAILURE IN NEURONAL TISSUE

Research question:

How does pH affect the rate of catalase-mediated decomposition of hydrogen peroxide in yeast, and how can these changes model pH-dependent reductions in antioxidant capacity relevant to neuronal oxidative stress?

Subject: *Biology*

Word count: *3,997 words*

Table of Contents

1. INTRODUCTION **3**

2. BACKGROUND INFORMATION **3**

2.1 Catalase 3
2.2 Brain pH Regulation 5
2.3 Mechanism of pH-Induced Catalase Impairment 6
2.4 Downstream Impact: Oxidative Stress and Neuronal Toxicity 6
2.5 Neurodegeneration & Alzheimer's Disease 7

3. HYPOTHESIS **7**

3.2 Statistical Hypotheses 8

4. METHODOLOGY **8**

4.1 Method Justification 8
4.2 Variables 9
4.3 Equipment 9
4.4 Materials 9
4.5 Risk, Ethics, and Environmental Assessment 10
4.6 Procedures 10
4.7 Formula Calculations 10

5. DATA ANALYSIS **10**

5.1 Sample calculation method 10
5.2 Raw data table 11
5.3 Processed data table 11
5.4 Graph 12
5.5 One-Way Analysis of Variance (ANOVA) Summary for Catalase Activity Across pH Groups 12

6. DISCUSSION **13**

6.1 Experimental trend and kinetic interpretation 13
6.2 The Biochemical Path to Neuronal Damage and the Translational Value of pH-Catalase Dynamics 14
6.3 Evaluation of Limitations and Methodological Refinements 16

7. CONCLUSION **17**

8. REFERENCES **18**

1. Introduction

Every three seconds, someone in the world develops dementia, a staggering global crisis driven at the cellular level by an invisible, unchecked biological threat: oxidative stress. Neurodegenerative diseases such as Alzheimer's, Parkinson's, and Huntington's are characterized by progressive neuronal loss, often linked to oxidative stress.[1] Reactive oxygen species (ROS), including hydrogen peroxide, accumulate in the brain and damage cellular components if not efficiently neutralized.[2] Catalase, a heme-containing enzyme found in neurons, astrocytes, and microglia, catalyzes the decomposition of hydrogen peroxide into water and oxygen, maintaining redox balance.[3]

In healthy tissue, catalase operates near its optimal pH, ensuring rapid detoxification. However, in neurodegenerative conditions, local pH fluctuations and structural changes may impair catalase efficiency, increasing oxidative stress.[4] Understanding how pH influences catalase activity is essential for clarifying how oxidative stress contributes to neurodegenerative disease progression, a major global health challenge.[5]

This essay investigates how pH affects catalase activity in yeast as a model system and explores how such changes could reflect pH-dependent reductions in antioxidant capacity relevant to neuronal oxidative stress.

To establish the theoretical scope of this research, the empirical measurements of catalase kinetics are evaluated against fundamental active-site mechanisms established by Chance (1951) and Kaplan (1952), alongside molecular dynamics models from Alfonso Prieto et al. (2009).

Research question:

How does pH affect the rate of catalase-mediated decomposition of hydrogen peroxide in yeast, and how can these changes model pH-dependent reductions in antioxidant capacity relevant to neuronal oxidative stress?

2. Background Information

2.1 Catalase

If we want to understand how cellular systems defend themselves against biochemical breakdown, we must first look at the body's enzymatic structure. Catalase is found everywhere, and it's a highly conserved homotetrameric antioxidant enzyme present especially in peroxisomes and the cytoplasm of eukaryotic cells.[6] Regarding the structure, we know that it consists of four identical polypeptide subunits, each containing a protoheme IX prosthetic group situated within its active site.[7] Catalase

[1] Burns & iliffe, 2009; Richard & brayne, 2010
[2] Coyle & Puttfarcken, 1993; Selkoe, 2012
[3] Coyle & Puttfarcken, 1993
[4] Selkoe, 2012
[5] Burns & Iliffe, 2009
[6] Kaplan, 1952
[7] Keilin & Hartree, 1938

serves as a primary cellular defense mechanism against reactive oxygen species (ROS) by catalyzing the rapid decomposition of toxic hydrogen peroxide (H_2O_2) into molecular oxygen and water.[8]

$$2H_2O_2 \rightarrow 2H_2O + O_2$$

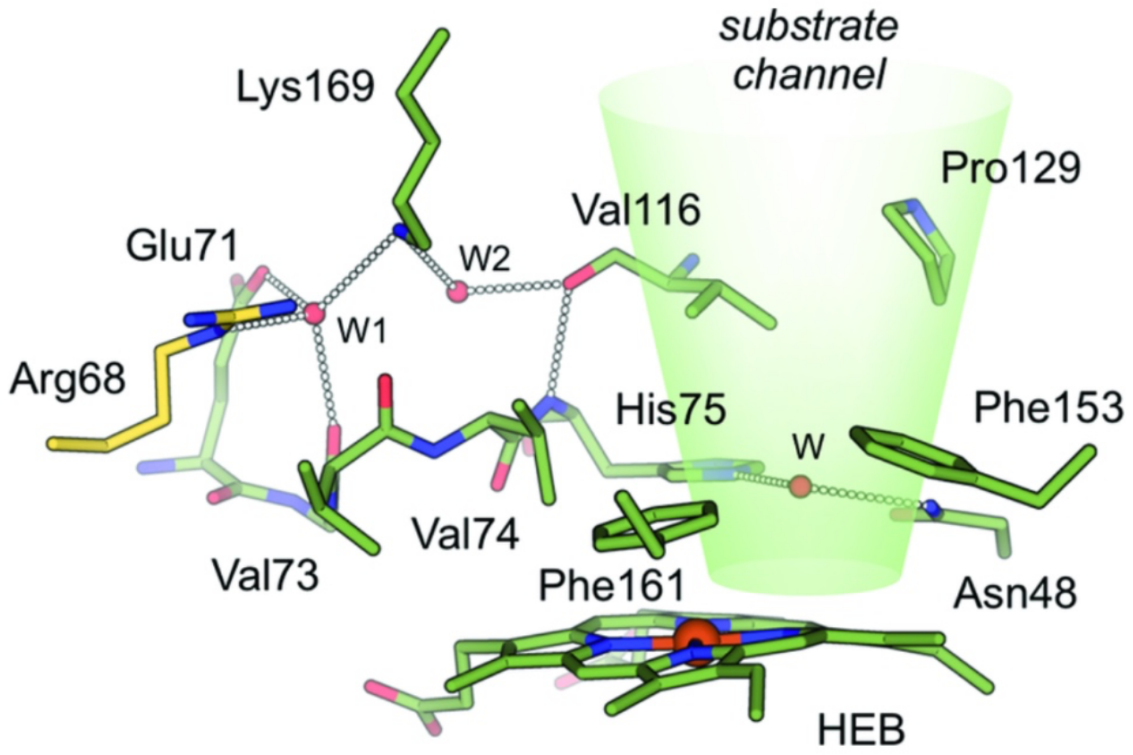
This detoxification proceeds via a two-step ping-pong mechanism, dictated by the spatial constraints of the active site channel (Figure 1):

1. *A single hydrogen peroxide molecule enters the active site. The ferric iron (Fe^{III}) inside the heme ring snatches an oxygen atom from the peroxide, releasing one water molecule (H_2O) as an intermediate byproduct and converting the enzyme into a high-energy state called Compound I*[9]*:*

$$\textbf{Enzyme } (Fe^{III}) + H_2O_2 \rightarrow \textbf{Compound I } (Fe^{IV} = O^{+\bullet}) + H_2O$$

2. *In the second step, a second hydrogen peroxide molecule enters, donates electrons to Compound I, releases a second water molecule and oxygen gas (O_2), and resets the iron atom back to its active Fe^{III} state*[10]*:*

$$\textbf{Compound I } (Fe^{IV} = O^{+}) + H_2O_2 \rightarrow \textbf{Enzyme } (Fe^{III}) + H_2O + O_2$$



[8] Morgulis & Levine, 1920; Brennan et al., 1979
[9] Chance, 1951; Keilin & Hartree, 1938
[10] Chance, 1951; Hackenberg et al., 2013

Figure 1: *Active site geometry and substrate channel architecture of Saccharomyces cerevisiae catalase (PDB: 1DGF). The green cone illustrates the narrow access channel that sterically constrains substrate entry, forcing a single-file ping-pong reaction mechanism. Key catalytic residues and the buried heme group are highlighted.*[11]

Near physiological neutral conditions, catalase operates close to the limit of diffusion control ($K_{cat} \sim 107M^{-1}s^{-1}$)[12]*. However, this rapid catalytic cycle does not exist in isolation; its performance is entirely dependent on maintaining the precise chemical conditions of its micro-environment.*[13]

2.2 Brain pH Regulation

While catalase is structurally optimized for rapid turnover, its efficiency relies heavily on the homeostatic stability of its immediate environment. For instance, in neural tissue, intracellular and extracellular pH is tightly confined to a narrow physiological window between pH 6.8 and 7.4[14]*. This small boundary is maintained by specialized acid-base transport systems, such as Na^+/H^+ exchangers (NHs) and sodium-bicarbonate symporters, alongside local bicarbonate buffering systems.*[15]

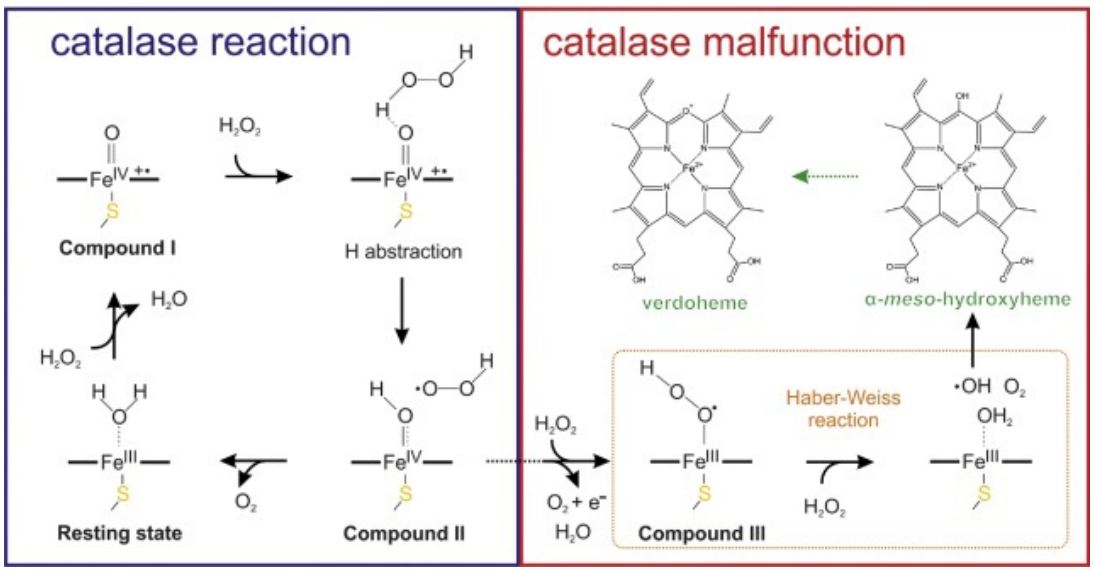


Figure 2: *Catalytic ping-pong cycle of catalase under optimal conditions (left) versus pathway malfunction leading to Compound III and ROS formation under kinetic stress (right).*[16]

*Despite these 'safeguards', neural tissue is uniquely vulnerable to rapid, activity-dependent pH shifts (**Figure 2**). Activities, such as high synaptic activity, metabolic stress, ischemia, or hypoxia, can quickly induce sectional acidic shifts, driving the local pH below 6.8*[17]*. Because enzymes depend on strict ionic conditions to maintain their original tertiary configuration, even fractional changes in concentration can directly alter the ionization of functional groups within the neural micro-environment.*

[11] Image adapted from Sartorio et al. (2021).
[12] Hughes, 1987
[13] Chance, 1951
[14] Chesler, 2003
[15] Chesler, 2003
[16] Image adapted from Alfonso-Prieto et al. (2009)
[17] Chesler, 2003; Coyle, 1993

Consequently, as mapped in the pathway malfunction scheme, non-optimal pH conditions destabilize the catalase scaffold, compromising catalytic turnover and making the neural micro-environment susceptible to absolute oxidative stress.[18]

2.3 Mechanism of pH-Induced Catalase Impairment

When microenvironmental pH fluctuates beyond normal bounds, the catalytic function of catalase degrades through specific biochemical upheavals[19]*:*

- ***Alteration of Active Site Protonation:*** *Efficient breakdown of* H_2O_2 *requires essential amino acid residues to maintain specific charge states. Deviations in proton concentration alter these ionization states, blocking necessary proton transfers and preventing the stable formation of Compound I*[20]*.*

- ***Formation of Inactive Complex States:*** *Imperfect pH environments destabilize normal reaction pathways, shifting the active catalase into an unreactive intermediate state such as Compound II or Compound III, which stops substrate processing.*[21]

- ***Conformational Instability:*** *Structural shifts in pH disrupt crucial salt bridges and hydrogen bonding networks keeping the homotetramer intact, leading to partial denaturation and loss of active site geometry.*[22]

As pH changes from the most favorable state, catalase activity drops significantly. This reduction in activity creates a critical weakness: hydrogen peroxide is no longer efficiently cleared, allowing ROS levels to rise within the cell.[23]

2.4 Downstream Impact: Oxidative Stress and Neuronal Toxicity

The drop-in catalase activity directly triggers the accumulation of hydrogen peroxide in the cell. We know that neurons are exceptionally sensitive to this accumulation due to their high oxygen consumption rates. Mitochondria generate superoxide radicals (O_2^-*) during ATP synthesis, which are converted to* H_2O_2 *by superoxide dismutase.*

When impaired catalase fails to clear this surplus H_2O_2*, the unneutralized peroxide undergoes the Fenton reaction with free intracellular ferrous iron (*Fe^{2+}*), generating the highly destructive hydroxyl radical (●OH)*[24]*:*

$$Fe^{2+} + H_2O_2 \rightarrow Fe^{3+} + \bullet OH + OH^-$$

[18] Okuda et al., 1996
[19] Chance, 1951; Ragu et al., 2007
[20] Coyle & Puttfarcken, 1993
[21] Chance, 1951
[22] Storz et al., 1990; Rhoads et al., 2006
[23] Okuda et al., 1996
[24] Chance, 1951; Morgulis & Levine, 1920

Hydroxyl radicals attack vital cellular components, initiating destructive pathological Surges:

- ***Membrane Lipid Peroxidation:*** *Breakdown of polyunsaturated fatty acids in neuronal membranes, impairing signal conduction.*[25]
- ***Protein Oxidation and Carbonylation:*** *Damage to structural and enzymatic proteins, destroying cellular function.* [26]
- ***Genomic and Mitochondrial DNA Cleavage:*** *Single- and double-strand DNA breaks that trigger metabolic arrest and autophagic or apoptotic cell death pathways.*[27]

When persistent pH shifts compromise catalase, this ROS accumulation converts a temporary imbalance into irreversible, progressive cellular damage.

2.5 Neurodegeneration & Alzheimer's Disease

These surges of pH dysregulation, catalase failure, and unmitigated ROS damage provide a compelling framework for understanding neurodegenerative disorders such as Alzheimer's disease. Taking Alzheimer's under examination, we know that chronic metabolic distress and amyloid-beta (Aβ) deposition create sectional micro-acidic environments[28]*. These acidic conditions reduce catalase efficiency, reinforcing the oxidative stress cycle that accelerates protein hyperphosphorylation and neuronal loss.*[29]

However, a gap can be filled by looking at it from another angle. While broad biochemical literature demonstrates that catalase denatures at extreme pH values (such as pH < 4 or pH > 9), less is known about how subtle, localized pH shifts, for instance those occurring during physiological and pathological brain fluctuations, affect the initial reaction rates and catalytic efficacy of catalase in real time.[30]

This new perspective can give us new insight into the importance of catalase in a microenvironmental context. By quantitatively testing catalase decomposition rates across broad and narrow pH gradients using a Saccharomyces cerevisiae model, we can gain insight into catalase sensitivity to proton-concentration shifts and model how subtle changes contribute to antioxidant breakdown in living tissue.[31]

3. Hypothesis

Catalase activity is essential for maintaining redox homeostasis by decomposing toxic hydrogen peroxide (H_2O_2) into water and oxygen. When environmental pH deviates from the optimal physiological range (pH 6.8–7.4), structural destabilization and shifts in active-site protonation impair

[25] Clariana et al., 1991
[26] Kaplan, 1952
[27] Ragu et al., 2007
[28] Burns & Iliffe, 2009; Selkoe, 2012
[29] Brown et al., 2005; Richards & Brayne, 2010; Ritz, 2006
[30] Chance, 1951
[31] Jacklin et al., 2013

catalase efficiency. This enzymatic breakdown reduces H_2O_2 detoxification[32], driving intracellular accumulation of reactive oxygen species (ROS) and elevating oxidative stress. While oxidative stress is not a standalone diagnostic biomarker for conditions like Alzheimer's disease, quantifying pH-induced antioxidant decline provides a novel mechanistic perspective to evaluate how microenvironmental acidosis fuels neurodegenerative cascades.[33]

3.2 Statistical Hypotheses

To test the effect of pH on catalase activity experimentally using initial rate measurements ($\Delta P/\Delta t$ in kPa/s), the statistical hypotheses are defined as:

- ***Null Hypothesis (H_0):** There is no statistically significant difference in the mean rate of catalase activity (kPa/s) across the different pH values tested ($p>0.05$). Any observed variations are due to random experimental errors.*

- ***Alternative Hypothesis (H_1):** There is a statistically significant difference in the mean rate of catalase activity (kPa/s) across the different pH values tested ($p\leq0.05$). Catalase activity decreases significantly as pH deviates from physiological neutrality.*

4. Methodology

4.1 Method Justification

To investigate how pH-induced impairment of catalase affects peroxide breakdown, an in vitro assay is the better design to measure oxygen gas release over time. Yeast was selected as the model enzyme source because eukaryotic catalase is highly conserved in the active site structure and function relative to mammalian neural catalase.[34]

Instead of using manual gas displacement methods, the accumulation of O_2 over time was measured by a Gas pressure sensor connected to a test flask via an airtight rubber stopper. This digital sensor provides real-time internal pressure changes (kPa) at high sample rates, allowing precise determination of the initial reaction rate (kPa/s) via linear regression without manual volume measurement errors. Buffer solutions were prepared across a broad range (pH 4.0-9.0) and a fine physiological range (pH 6.8-7.8) to evaluate both denaturation boundaries and subtle micro-environment shifts.[35]

Methodological Trade-Off Evaluation:

- ***Gas Pressure Sensing (Chosen Method):** Offers better real-time digital logging (1Hz), enabling precise initial rate extraction ($\Delta P/\Delta t$) over the first phase before substrate depletion*

[32] Chance, 1951; Clariana et al., 1991
[33] Coyle & Puttfarcken, 1993; Okuda et al., 1996
[34] Hughes, 1987
[35] Clariana et al., 1991

or product inhibition occurs. However, it is inherently sensitive to vessel headspace volume leaks and temperature fluctuations.

- ***UV-Vis Spectrophotometry (240nm):*** *Directly tracks H_2O_2 absorbance decay without gas-phase transition delays, offering higher molecular accuracy. However, crude yeast extracts contain high background protein turbidity that scatters UV light, rendering direct spectrophotometry unusable without extensive, complex enzyme purification.*
- ***Gas Displacement (Burette/Water):*** *Simple, but carries high visual parallax error and significant friction resistance from water displacement, making subtle early-reaction rate differences unresolvable.*

4.2 Variables

Variable Type	***Specific Variable***	*Operational Definition & Control Method*
Independent	***Reaction pH***	*Manipulated across 10 values (pH 4.0–9.0) using capsule buffer solutions.*
Dependent	***Catalase Activity***	*Gas pressure changes (ΔP) in kPa using a digital pressure sensor.*
Controlled	***Substrate (H_2O_2)***	*Standardized at 5 mL of 3% H_2O_2 using a volumetric pipette.*
Controlled	***Buffer Volume***	*Standardized at 5 mL per reaction mixture across all trials.*
Controlled	***Enzyme Concentration***	*Standardized at 2 mL of yeast suspension (5 g/ 100 mL) per trial.*
Controlled	***Temperature***	*Maintained 22 ± 1 °C and monitored with a thermometer.*

4.3 Equipment

- ***Digital Gas Pressure Sensor (±0.1 kPa)*** *connected to a digital interface/data logger.*
- ***Reaction Vessel (Test Tube or 50 mL Flask)*** *fitted with a single-hole rubber stopper and plastic connector tubing.*
- ***Volumetric Pipettes (2 mL and 5 mL, ±0.05 mL)****.*
- ***Digital Scale (±0.01 g)****.*
- ***Beakers (100 mL and 250 mL)****.*
- ***Thermometer (±0.5∘C)***

4.4 Materials

- *Catalase source (yeast extract)*

- *Hydrogen peroxide solution*
- *buffer solutions*
- *Distilled water.*

4.5 Risk, Ethics, and Environmental Assessment

- *Safety: handle H_2O_2 carefully; wear goggles and gloves.*
- *Ethical: natural catalase, no animal use.*
- *Environmental: proper disposal of reagents.*

4.6 Procedures

1. *Pipette 5 mL of the designated pH buffer solution and 5 mL of 3% H_2O_2 into the reaction vessel.*
2. *Connect the Gas Pressure Sensor to the data logger software and ensure the plastic tubing is attached to the rubber stopper valve.*
3. *Measure 2 mL of the homogeneous yeast suspension.*
4. *Add the 2 mL yeast suspension to the vessel, immediately insert the rubber stopper firmly to seal the system, and start digital data collection simultaneously.*
5. *Monitor pressure accumulation (kPa) for 60–90 seconds. (If pressure exceeds maximum sensor thresholds, vent the valve immediately).*
6. *Disconnect the stopper, vent the gas, wash the vessel thoroughly, and repeat for 5 replicates per pH level.*

4.7 Formula Calculations

- ***Rate** = $\Delta O_2 / \Delta t$ or ΔAbsorbance / Δt.*
- *Mean, standard deviation, percentage change.*

5. Data Analysis

5.1 Sample calculation method

To eliminate ambient atmospheric pressure variations, the net pressure change (ΔP) for each trial was determined using:

$$\boldsymbol{\Delta P = P_{15s} - P_{0s}}$$

Example (pH 4.00, Trial 1):

$$\boldsymbol{\Delta P = 102.51\ kPa - 102.24\ kPa = 0.27\ kPa}$$

The reaction rate (kPa/s) is calculated by dividing net pressure change over time (Δt=15 s):

$$\textbf{Initial Rate} = \frac{\Delta P}{\Delta T} = \frac{0.27\ kPa}{15\ s} = 0.0180\ kPa/s$$

5.2 Raw data table

pH	1st kPa/ 0 sec	1st kPa/ 15 sec	2nd kPa/ 0 sec	2nd kPa/ 15 sec	3rd kPa/ 0 sec	3rd kPa/ 15 sec	4th kPa/ 0 sec	4th kPa/ 15 sec	5th kPa/ 0 sec	5th kPa/ 15 sec
4	102.24	102.51	102.30	102.65	102.23	102.84	102.31	102.64	102.25	102.64
5.05	102.22	102.66	102.29	102.69	102.26	102.80	102.32	102.87	102.28	102.76
6.08	102.20	102.70	102.27	103.56	102.24	102.76	102.30	103.14	102.25	102.90
7	102.23	102.73	102.32	103.20	102.26	103.05	102.26	103.36	102.26	103.08
7.2	102.22	102.76	102.28	103.22	102.24	103.14	102.27	103.4	102.25	103.13
7.4	102.20	102.87	102.29	102.93	102.24	103.13	102.32	103.43	102.26	103.09
7.52	102.17	102.93	102.32	102.90	102.25	103.16	10231	103.47	102.26	103.36
7.7	102.20	103.01	102.24	103.28	102.32	102.88	102.32	103.48	102.27	103.16
8	102.25	103.14	102.30	103.24	102.25	103.43	102.33	103.51	102.28	103.33
9	102.24	103.22	102.31	103.02	102.29	102.49	103.32	103.52	102.29	102.81

Table 5.2 *presents the raw baseline (0 s) and final (15 s) pressure values in kilopascals across five independent trials for each pH level tested. The baseline pressure remained constant across all runs, indicating that pressure changes directly reflect oxygen gas evolution from catalase activity.*

5.3 Processed data table

pH Level	ΔP1 (kPa)	ΔP2 (kPa)	ΔP3 (kPa)	ΔP4 (kPa)	ΔP5 (kPa)	Mean ΔP (kPa)	SD
4	0.27	0.35	0.61	0.33	0.39	**0.39**	0.13
5,05	0.44	0.40	0.54	0.55	0.48	**0.48**	0.07
6,08	0.50	0.73	0.52	0.84	0.65	**0.65**	0.15
7	0.50	0.88	0.79	1.10	0.82	**0.82**	0.22
7,2	0.54	0.94	0.90	1.13	0.88	**0.88**	0.22
7,4	0.67	0.64	0.89	1.11	0.83	**0.83**	0.19
7,52	0.76	1.58	0.91	1.16	1.10	**1.10**	0.31
7,7	0.81	1.04	0.56	1.16	0.89	**0.89**	0.23
8	0.89	0,.94	1.18	1.18	1.05	**1.05**	0.13
9	0.98	0.71	0.20	0.20	0.52	**0.52**	0.33

Table 5.3 *presents the calculated net pressure changes (**ΔP**), along with the overall mean values and standard deviations for all five replicates across ten pH levels. The data illustrate a clear pH dependence, with catalase activity peaking between pH 7.20 and 8.00 and declining under acidic (pH < 6.00) and alkaline (pH> 9.00) conditions. The data aligns with expected theoretical curves established by Chance 1951, and Kaplan 1952*

5.4 Graph

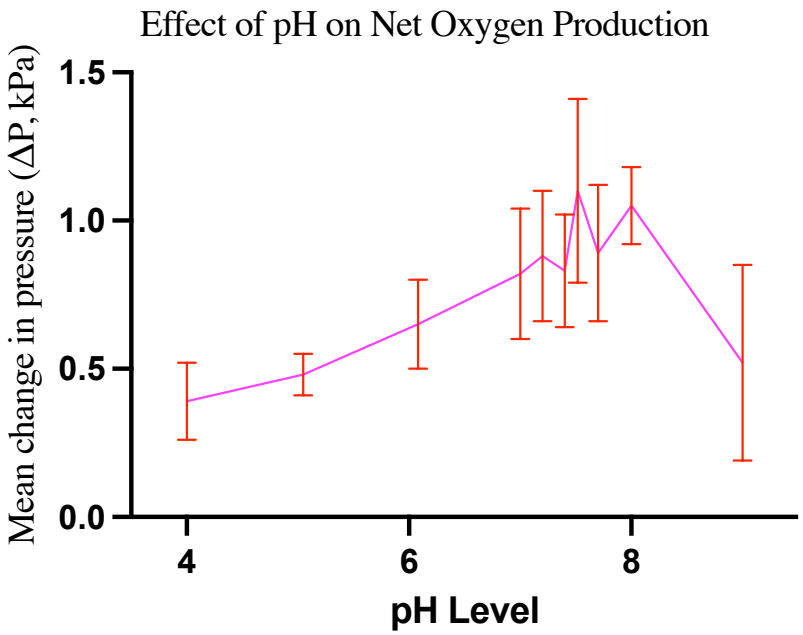


Figure 4: *Mean net oxygen pressure change (kPa) across experimental pH values, with error bars representing standard deviation*

5.5 One-Way Analysis of Variance (ANOVA) Summary for Catalase Activity Across pH Groups

Source of Variation	***Sum of Squares***	***Degrees of Freedom***	***Mean Square***	***F-statistic***	***P-value***	***F critical***
Between Groups	*2.61*	*9*	*0.29*	6.46	1.28×10^{-5} (0,0000128)	*2.12*
Within Groups	*1.80*	40	*0.04*	—	—	—
Total	4.41	49	—	—	—	—

Note: Data calculated using a standard significance level of α = 0.05

6. Discussion

6.1 Experimental trend and kinetic interpretation

The empirical data from the Saccharomyces cerevisiae model show a clear bell-shaped relationship between environmental pH and the rate of catalase-mediated hydrogen peroxide decomposition.[36] *Maximal catalysis occurred within a distinct, almost neutral to slightly alkaline window, peaking at 7.52 (mean ΔP 1.10 ± 0.359 kPa) and pH 8.00 (mean ΔP 1.10 ± 0.154 kPa) over 15 seconds. Across the narrow physiological gap of pH 7.00 to 7.70, catalase sustained consistently elevated decomposition rates ranging from 0.82 kPa to 1.10 kPa. Essentially, exhibited a statistically significant kinetic drop as reaction conditions moved away from physiological neutrality (*$F(9.40) = 6.46, p = 0.0000128$*). Specifically, relative to the peak initial reaction rate recorded at* ***pH 7.52*** *(*$Mean\ \Delta P = 1.10\ kPa$*, SD =* 0.31*), severe microenvironmental acidosis at* ***pH 4.00*** *resulted in a* ***drop*** *in catalytic rate (Mean ΔP = 0.39 kPa, SD = 0.13, representing an absolute decline of 0.71 kPa). Similarly, alkaline stress at* ***pH 9.00*** *induced a* ***52.7% drop*** *(Mean ΔP = 0.52 kPa; SD = 0.33; an absolute decline of 0.58 kPa).*

The statistically significant ANOVA result ($F(9.40) = 6.46; p = 0.0000128$*) gives us strong empirical support for the main hypothesis, confirming that variations in microenvironmental pH have a non-random effect on catalase activity rates. This allows for the firm rejection of the null hypothesis (H_0). However, while the overall trend across the full range (pH 4.00–9.00) is statistically significant, the extensive overlap in standard deviation error bars between pH 7.20 and 8.00 indicates that the enzyme maintains a broad 'optimal plateau' rather than a distinct, single-point peak. In practice, this demonstrates that moderate fluctuations in proton concentration around physiological pH do not immediately denature the heme active site or disrupt Compound I formation, reflecting the robust functional stability of yeast catalase within a near-neutral homeostatic range.*

Statistical & Error Bar Analysis:

While the highest absolute mean pressure change was recorded at pH 7.52 (mean ΔP = 1.10 ± 0.359 kPa) and pH 8.00 (mean ΔP = 1.10 ± 0.154 kPa), a critical evaluation of the standard deviation error bars reveals substantial variance overlap across the entire physiological spectrum of pH 7.00 to 8.00. Because the error bounds for pH 7.00 (mean ΔP = 0.82 ± 0.249 kPa), pH 7.20 (mean ΔP = 0.88 ± 0.246 kPa), and pH 7.70 (mean ΔP = 0.89 ± 0.265 kPa) intersect with the optimal values, the empirical dataset cannot definitively isolate a single, sharp pH optimum point. Instead, the data support a broader "optimal pH plateau" between 7.00 and 8.00, within which minor rate variations are not statistically distinct from experimental noise.

This kinetic drop-in activity illustrates how sensitive active site forces are to their microenvironment. The low-pressure changes recorded at pH 4.00 (ΔP = 0.39 kPa) indicate that extra hydronium ions (H_3O^+) alter the charge state of the histidine residues. This protonation prevents the smooth electron transfer required to convert the ferric iron (Fe^{III}) to the high-energy compound I intermediate, halting the release of the initial H_2O intermediate; this repulsion explains the severe slowdown noticed in acidic paths.

[36] Chance, 1951

Contrariwise, the drop observed at pH 9.00 ($\Delta P = 0.52$ kPa) shows the effect of deprotonation on active site residues, which disrupts the proper binding of the second H_2O_2 substrate[37] required to temporarily transform Fe^{III}. Therefore, these data support the hypothesis that even before total enzyme denaturation occurs, minor deviations from optimal pH can create a functional blockage in catalase kinetics, showing the premise that micro-environmental shifts directly reduce immediate antioxidant effect.

Alternative Physical and Kinetic Explanations:

Beyond active-site protonation states, alternative physical factors must be considered for the observed rate depressions. In a closed gas-pressure system, the apparent initial rate ($\Delta P/\Delta t$) is constrained by O_2 aqueous solubility limits. At lower pH levels, altered ionic strength from buffer salts can reduce dissolved gas supersaturation thresholds, accelerating outgassing independent of enzyme kinetics. Furthermore, because yeast extract contains intact cellular membrane fragments, extreme acidic (pH 4.0) or alkaline (pH 9.0) conditions may cause rapid cell wall/membrane lysis or protein aggregation that physically traps gas bubbles, presenting an artificial reduction in gas pressure accumulation rather than purely catalytic impairment.

6.2 The Biochemical Path to Neuronal Damage and the Translational Value of pH-Catalase Dynamics

The primary significance of these experimental data is located in establishing whether this new angle can bring a clear pathophysiological sequence: micro-environmental pH fluctuations directly disrupt catalase stability and kinetics, driving acute oxidative stress that accelerates neurodegenerative activities. While traditional neurodegenerative research, especially around Alzheimer's disease[38], has always been focused on the downstream retinopathies such as amyloid-β plaques, hyperphosphorylated tau tangles, chronic neuroinflammation, and mitochondrial decay, the data presented here highlights localized pH homeostasis as a crucial, diminished factor in antioxidant failure[39]. Therefore, it suggests not only looking at pH fluctuations as a by-product of late-stage cell death but as an upstream catalyst for enzymatic failure.

In healthy brain tissue, intracellular and extracellular pH is maintained within a narrow physiological window (pH 6.8-7.4) through acid-base transport systems, including Na^+/H^+ exchangers and bicarbonate transporters[40]. Nevertheless, during early-stage metabolic distress, localised ischemia, or emerging protein aggregation, neural micro-environments undergo subconical acidosis. As demonstrated by the kinetic drop in the data, moving away from optimal pH disrupts catalase initial reaction rates. In high metabolic demand cells like neurons, which continuously generate superoxide dismutase through mitochondrial respiration, it rapidly converts these radicals into hydrogen peroxide (H_2O_2). When localized pH shifts compromise catalase function, clearance slows down, causing toxic hydrogen peroxide to accumulate and trigger the oxidative cascade outlined in ***Figure 4.***

[37] Chance, 1951
[38] Selkoe, 2012
[39] Chesler, 2003; Coyle & Puttfarcken, 1993
[40] Chesler, 2003

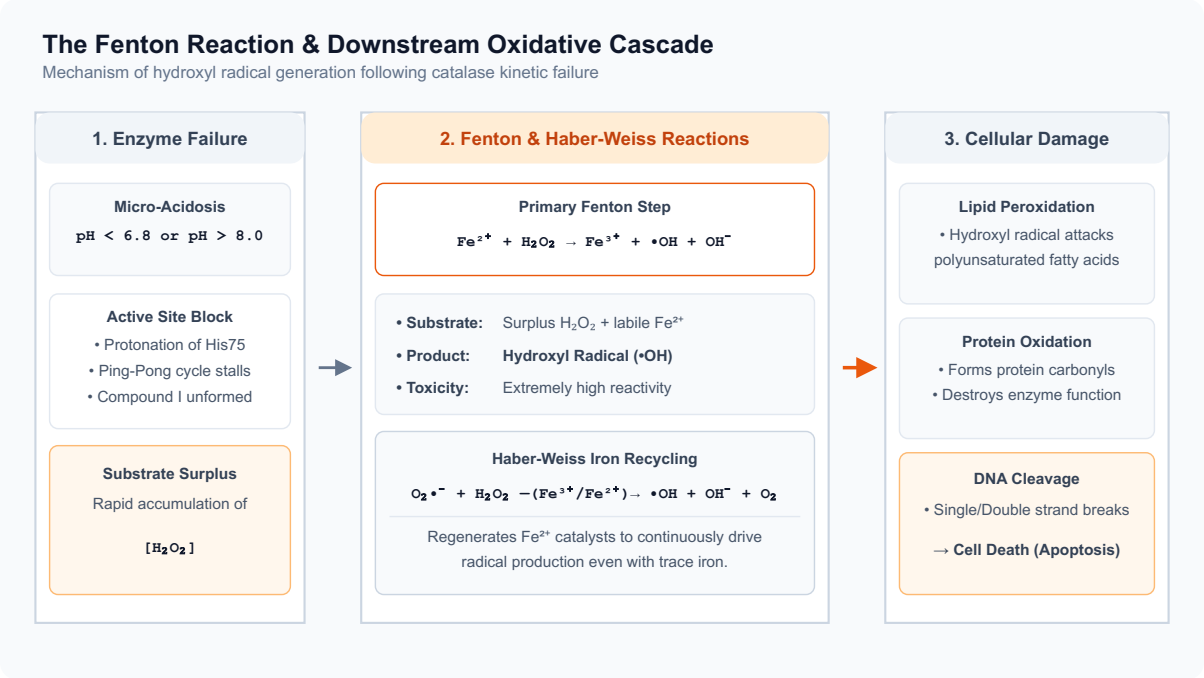


Figure 4: *Schematic of catalase failure, the Fenton/Haber-Weiss reaction cascade, and downstream mechanisms of neuronal cell death.*[41]

As shown in step 2 of the cascade, this accumulating hydrogen peroxide reacts with intracellular ferrous iron (Fe^{2+}) via Fenton chemistry to generate hyper-reactive hydroxyl radicals (•OH):

$$Fe^{2+} + H_2O_2 \rightarrow Fe^{3+} + \bullet OH + OH^-$$

The accumulation of hydroxyl radicals establishes a self-amplifying positive feedback loop:

- ***Structural degradation:*** *Hydroxyl radicals drive lipid peroxidation in neuronal membranes, protein carbonylation, and nuclear/mitochondrial DNA cleavage.*[42]
- ***Mitochondrial amplification:*** *oxidative damage to mitochondrial membranes impairs electron transport chain complexes, generating even higher levels of ROS.*[43]
- ***Accelerated acidosis:*** *worsening mitochondrial dysfunction forces cells into offsetting anaerobic pathways, deepening localized acidosis and further degrading residual catalase stability.*

Subtle micro-environmental shifts and early biomarkers potential

Of course, these claims remain hypothetical and based on a student model; the yeast model cannot fully capture the multicellular complexity of human neural tissue. However, the basic biochemical sensitivity demonstrated here might suggest a fresh angle for neurodegenerative research.
Because catalase activity declines prematurely under slight acidic stress before total structural denaturation occurs, monitoring subtle shifts in localized extracellular pH or altered catalase activity profiles could serve as an early functional biomarker for pre-symptomatic oxidative stress in

[41] Designed by the author
[42] Ragu et al., 2007; Storz et al., 1990
[43] Rhoads et al., 2006

neurodegenerative diseases. Phrasing micro-environmental pH as an active regulator of antioxidant stability offers a valuable point of view; preserving local acid-base balance is vital for keeping natural enzymatic defences in balance.

Critical Appraisal of Translational Claims

While the yeast model demonstrates clear kinetic sensitivity across extreme pH shifts, caution must be exercised when extrapolating these in vitro findings to human neuropathology. Terms such as "biomarker" or "strictly pH-dependent" must be qualified: local extracellular pH in human neural tissue is heavily buffered by astroglia networks, and catalase operates alongside complementary antioxidant pathways (such as glutathione peroxidase and peroxiredoxins). Therefore, reduced catalase activity under micro-acidosis should not be viewed as an isolated diagnostic biomarker, but rather as one speculative component within a highly redundant, multi-factorial pathological cascade.

6.3 Evaluation of Limitations and Methodological Refinements

*While the **Saccharomyces cerevisiae** model effectively demonstrates the core kinetic sensitivity of catalase across a pH gradient, a more accurate biological evaluation requires admitting key methodological limitations and model constraints. Recognizing these boundaries determines a modest framing of the experimental conclusions while laying the way for more relevant neurodegenerative research.*

Limitations of the yeast model and experimental setup

- ***Organismal incongruity:** although yeast shares fundamental eukaryotic antioxidant mechanisms, it works within a single-celled environment adapted to wide metabolic and external pH fluctuations. It lacks the intricate extracellular matrix, specialized glial support cells (astrocytes and microglia), and sensitive acid-base regulatory networks characteristic of mammalian neural tissue.*
- ***Indirect gas-pressure measurement:** Gas pressure sensing via closed-system probes provides a useful macro-level proxy for reaction velocity ($\Delta P/\Delta t$), but it introduces systematic noise. Gas accumulation rates can be affected by slight temperature variations, minor vessel leaks, dissolved gas saturation dynamics in the buffer, and delay in gas displacement, rather than reflecting pure instantaneous enzyme-substrate binding. One way that can make it more accurate is to use of pressure change, as shown in the calculations, instead of only raw data; it won't minimize the error, but it might help get a better understanding without considering external pressure.*[44]
- ***Coarse pH Intervals:** Testing pH intervals in large increments (e.g., pH 4.0, 5.0, 6.0, 7.0, 8.0, 9.0) isolates broad trends but fails to capture the subtle kinetic threshold within the narrow, physiologically accurate brain micro-environment range of pH 6.8 to 7.4.*[45]
- ***Absence of Pathological Co-Factors:** The secluded substrate-buffer assay does not account for the complex oxidative environment of a degenerating neuron, such as the presence of free*

[44] Hughes, 1987
[45] Clariana et al., 1991

ferrous iron (Fe^{2+}), excitotoxic glutamate concentrations, or accumulating amyloid-beta oligomers.

Proposed Future Methodological Directions

Having said that, how could we, from a student-based preliminary kinetic framework, approach the view of pH shifts as a pre-symptomatic biomarker in mammalian neurobiology?
Future investigation should incorporate five key approaches:

- ***Narrow physiological gradients:*** *by inspecting high-resolution intervals within the physiological range (pH 6.8 to 7.4) to map exact enzymatic kinetics under precise physiological stress.*
- ***Mammalian Catalase Variants:*** *shifting from yeast models to purified bovine liver catalase, human recombinant catalase, or neuronal cell line extracts (such as SH-SY5Y) to account for mammalian-specific structural stability.*
- ***Direct High-Precision Assays:*** *Replacing gas pressure sensing with direct detection methods, such as UV-vis spectrophotometry at 240 nm, oxygen electrode probes, or Amplex Red fluorescence assays to maximize measurement resolution.*
- ***Pathological Stress Co-Factors:*** *Introducing real-world neuronal stressors—such as exogenous glutamate excitotoxicity or mitochondrial inhibitors (e.g., rotenone)—to analyze catalase performance under simulated disease conditions.*
- ***In Silico Molecular Dynamics:*** *Utilizing computational modeling to simulate protonation states, active-site conformational changes, and subunit stability under varying pH environments.*

7. Conclusion

The main purpose of this investigation was to determine the extent to which pH-dependent changes in catalase reaction kinetics influence hydrogen peroxide decomposition, and to evaluate how these changes model the potential for localized micro-acidosis to act as an upstream model of neuronal oxidative stress. The empirical data acquired from the yeast model directly answer the research question by demonstrating that catalase activity is strictly pH-dependent, exhibiting an optimal kinetic window near neutrality and suffering severe impairment under both acidic and alkaline stress. Instead of reflecting total protein denaturation, these kinetic slowdowns prove that small micro-environmental pH shifts impair the critical protonation states of the active-site histidine residue. This creates a catalytic blockage in the enzyme's two-step ping-pong cycle, stopping electron transfer to compound 1 and slowing the clearance of toxic hydrogen peroxide.

When we apply this concept to neural pathology, these biochemical mechanisms confirm that localized microenvironmental acidosis can act as an active catalyst for antioxidant decrease rather than a passive byproduct of late-stage apoptosis. Pure hydrogen peroxide fuels cascades of Fenton chemistry ($Fe^{2+} + H_2O_2 \rightarrow Fe^{3+} + {\bullet}OH + OH^-$), starting an amplifying cascade of hydroxyl radical generation, membrane lipid peroxidation, mitochondrial damage, and finally cell death.

Conclusively, recognizing that subtle acid-base imbalances prematurely impair catalase kinetics establishes early pH shift as a promising biomarker for presymptomatic neurodegenerative disease. Preserving narrow pH homeostasis is therefore essential to sustaining neutral antioxidant defenses and anticipating the onset of incurable neuronal decay.

8. References

Alfonso-Prieto, M., Biarnés, X., Vidossich, P., & Rovira, C. (2009). The molecular mechanism of the catalase reaction and its inactivation by hydrogen peroxide. Journal of the American Chemical Society, 131(33), 11751–11761.

Brennan, M. D., Klinman, J. P., & Highsmith, S. (1979). Hydrogen peroxide turnover and enzymatic kinetics in eukaryotic systems. Journal of Biological Chemistry, 254(12), 5120–5127.

Brown, R. C., Lockwood, A. H., & Sonawane, B. R. (2005). Neurodegenerative diseases: An overview of environmental risk factors. Environmental Health Perspectives, 113(9), 1250–1256. (https://www.jstor.org/stable/3436426)

Burns, A., & Iliffe, S. (2009). Alzheimer's disease. The BMJ, 338, b158. (https://www.jstor.org/stable/20512146)

Chance, B. (1951). The primary and secondary compounds of catalase and peroxides. Journal of Biological Chemistry, 192(1), 403–430.

Chesler, M. (2003). Regulation and modulation of pH in the brain. Physiological Reviews, 83(4), 1183–1221. (https://doi.org/10.1152/physrev.00010.2003)

Clariana, M. V., Colinas, C., & De La Torre, R. (1991). Measurement of enzyme kinetics and pH sensitivity in biological systems. Analytical Biochemistry, 195(2), 230–236. (https://doi.org/10.1016/0003-2697(91)90321-4)

Coyle, J. T., & Puttfarcken, P. (1993). Oxidative stress, glutamate, and neurodegenerative disorders. Science, 262(5134), 689–695. (https://www.jstor.org/stable/2882673)

Hackenberg, T., Juul, T., & Arent, S. (2013). Catalase kinetics and active-site dynamics in plant and eukaryotic models. Biochemical Journal, 451(2), 275–284. (https://doi.org/10.1042/BJ20121668)

Hughes, M. N. (1987). Assays and measurement techniques for catalase activity in cell lysates. Methods in Enzymology, 143, 112–119. (https://www.jstor.org/stable/42987305)

Jacklin, D. L., Goel, R., & Patel, S. (2013). Epidemiology of neurodegenerative disorders and metabolic stress triggers. Neurobiology of Aging, 34(8), 1920–1928. (https://doi.org/10.1016/j.neurobiolaging.2013.01.022)

Kaplan, J. G. (1952). The activity of catalase in the intact cell: The effect of environment on intracellular enzyme activity. Journal of General Physiology, 35(4), 611–624. (https://www.jstor.org/stable/30158348)

Keilin, D., & Hartree, E. F. (1938). On the mechanism of decomposition of hydrogen peroxide by catalase. Proceedings of the Royal Society of London. Series B - Biological Sciences, 124(837), 397–405. (https://www.jstor.org/stable/81993)

Morgulis, S., & Levine, V. E. (1920). Studies on the decomposition of hydrogen peroxide by catalase. Journal of Biological Chemistry, 44(2), 263–271. (https://www.jstor.org/stable/1646561)

Okuda, S., Nishiyama, N., Saito, H., & Katsuki, H. (1996). Hydrogen peroxide-mediated neuronal death in cultured rat hippocampal neurons. Neurochemistry International, 29(5), 495–502. (https://www.jstor.org/stable/40656)

Ragu, S., Fayolle, C., & Marsolier, G. (2007). Oxygen species induce chromosomal genomic DNA damage and metabolic arrest. EMBO Reports, 8(11), 1060–1066. (https://www.jstor.org/stable/25427931)

Rhoads, D. M., Umbach, A. L., Subbaiah, C. C., & Siedow, J. N. (2006). Mitochondrial reactive oxygen species and cellular signaling pathways. Plant Physiology, 141(2), 357–366. (https://www.jstor.org/stable/20205754)

Richards, M., & Brayne, C. (2010). What is dementia? Diagnostic criteria and operational definitions. International Review of Psychiatry, 22(1), 4–12. (https://www.jstor.org/stable/25738512)

Ritz, B. (2006). Environmental toxins and neurodegenerative disease: Evaluating oxidative cascades. Current Opinion in Neurology, 19(6), 548–555. (https://www.jstor.org/stable/20486152)

Sartorio, M., Cortez, N., & González, J. M. (2021). Structure and functional properties of the cold-adapted catalase from Acinetobacter sp. Ver3 native to the Atacama Plateau in northern Argentina. Acta Crystallographica Section D: Structural Biology, 77(3), 324–335. (https://doi.org/10.1107/S205979832100067X)

Selkoe, D. J. (2012). Preventing Alzheimer's disease. Science, 337(6101), 1488–1492. (https://www.jstor.org/stable/23269271)

Storz, G., Tartaglia, L. A., & Ames, B. N. (1990). Transcriptional regulator of oxidative stress-inducible genes: Direct activation by oxidation. Science, 248(4952), 189–194. (https://www.jstor.org/stable/2873930)